Structure and electrical conductivity in fluid high-density hydrogen



1997 J. Phys.: Condens. Matter 9 11023

(http://iopscience.iop.org/0953-8984/9/50/008)

J. Phys.: Condens. Matter **9** (1997) 11023–11034. Printed in the UK PII: S0953-8984(97)83260-2

# Structure and electrical conductivity in fluid high-density hydrogen

O Pfaffenzeller† and D Hohl†‡

† Institut für Festkörperforschung, Forschungszentrum Jülich, D-52425 Jülich, Germany
‡ Department of Chemistry, Stanford University, Stanford, CA 94305, USA

Received 8 April 1997, in final form 28 August 1997

**Abstract.** We present an *ab initio* Hohenberg–Kohn–Sham density functional study of structure and electrical conductivity $\sigma$ in hot dense hydrogen. Our study covers the density range 0.40–1.34 mol cm$^{-3}$ ($r_s$ = 1.5–1, $P$ = 1.5–24 Mbar) at temperatures $T$ = 800–3000 K. In this range both a molecular–atomic and an insulator–metal transition are expected to take place. Our results are compared with recent double-shock experiments in the hot fluid phase. We observe an increase in $\sigma$ of an order of magnitude between $r_s = 1.5$ and 1. At the lowest density, hydrogen is a molecular liquid below about 1100 K and continuously atomizes with increasing $T$. At the highest density, the sample is a monatomic liquid metal with high coordination number at all $T$. The metallic fluid is atomic, not molecular, for all densities investigated.

## 1. Introduction

The prospect of turning hydrogen, the lightest of all elements, into a metal has fascinated physicists for many decades [1]. The energy difference of approximately 10 eV between insulating and conducting states would require on the order of 10 Mbar pressure to be overcome by mechanical work. Alternatively, temperatures around 100 000 K could accomplish metallization. Two strategies are currently being pursued to make metallic hydrogen.

Static high-pressure application at low temperatures in diamond anvil cells has reached the 2 Mbar mark [2]. One is limited to indirect optical methods to infer structure and conductivity in extremely small samples, and definitive results are difficult to obtain [3]. It is therefore unclear from an experimental point of view whether the current maximum-pressure phase ('H–A' or 'phase III') is metallic, atomic, both or neither. One can put a lower bound of 1.5 Mbar on the low-$T$ metallization pressure. Incidentally, this implies that metallic hydrogen will have a much higher specific weight (>0.8 g cm$^{-3}$) than lithium, the 'true' lightest of all metals.

Dynamical (multiple-) shock experiments generate Mbar pressures at several thousand kelvin temperatures, and are more interesting from an applications point of view. They probe the behaviour of the material under conditions of inertial confinement fusion experiments and in the interiors of planets, stars and other astrophysical objects. Very recently, metallization was indeed accomplished in the fluid phase using this elegant method [4, 5]. The experimental data show no evidence for a non-continuous first-order transition [6]. The authors of this work [4, 5] also claim, on the basis of a parametrized free energy model of an ideal mixture of $H_2$ molecules and H atoms with necessarily crude approximations [7],

0953-8984/97/5011023+12$19.50  

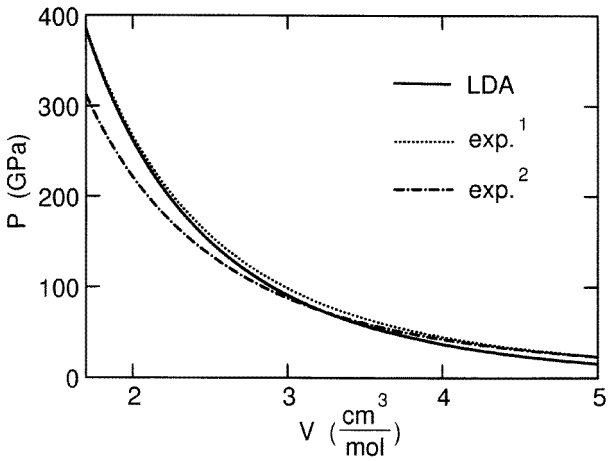


**Figure 1.** Pressure–volume relationship $P(V)$ for solid molecular hydrogen. The specific volume range shown is $V = 1.69$–$5.0$ cm$^3$ mol$^{-1}$ ($r_s = 1.3$–$1.86$). Solid line: present calculations at $T = 0$ K ('electronic' pressures only). Dotted line (1): measurement given in [8]. Dash-dotted line (2): measurement given in [9]. In our calculations density is the independent variable. We have calculated the pressures as function of density $P(\rho)$ by explicit $E_{tot}(\rho)$ calculations in small unit cells with four molecules, optimizing all geometrical parameters and fitting the results to a Birch–Murnaghan [8] equation of state ($V_0 = 23.0$ cm$^3$ mol$^{-1}$, $K_0 = 0.182$ GPa, $K_0' = 5.35$ and $K_0 K_0'' = 7.06$). Our calculated pressures are in good agreement with experiment and less than ∼8% higher than measured in the solid [9] for, e.g. $r_s \geqslant 1.5$. Note, however, that the experimental pressures in the fluid phase are significantly higher at the same density (∼120 GPa [4] and ∼70 GPa [9] in the fluid and solid phases, respectively, at 3.2 cm$^3$ mol$^{-1}$). Thermal pressure differences (⩽15 GPa) are not the major cause of this effect. In the shock experiments pressure $P$ and temperature $T$ are measured and the density $\rho$ is extracted from a model EOS. [4] cites a probable error of <5% in the resulting 'experimental' $\rho$ values (the uncertainties in $T$ are likely to be larger than this). Our $P$–$V$ conversion is based on the molecular solid. At $P = 1.5$ Mbar our computer sample has a higher density (0.40 mol cm$^{-3}$) than the fluid in the experiment [4] (0.34 mol cm$^{-3}$).

that the sample at the metallization point is basically *not* dissociated (atomic) but molecular. Our *ab initio* simulations lead to the reverse conclusion.

The calculations presented here address the $P/T$ domain of astrophysical objects and shock experiments. AC and DC conductivities are computed at fixed densities of $\rho = 0.40$, 0.59 and 1.34 mol cm$^{-3}$ (electron sphere radius parameter $r_s = 1.5$, 1.3 and 1.0; $r_s a_0 = (3V_e/(4\pi))^{1/3}$, where $a_0$ is the Bohr radius and $V_e$ is the volume per electron). This corresponds to calculated pressures within our model of $P = 1.5$, 3.8 and 24 Mbar, respectively (see figure 1). The temperatures were varied between 800 K and 3000 K. In plasma physics language, all our calculations were carried out deep in the 'strong coupling' regime. The dimensionless ion coupling parameter $\Gamma = Ze^2/(r_s k_b T)$ ranged from 100 ($r_s = 1$, $T = 3000$ K) to 244 ($r_s = 1.5$, $T = 800$ K). Likewise, the electronic system is deep in the quantal domain, with $\theta = T/T_F \ll 1$ ($T_F$ is the Fermi temperature of the fully degenerate non-interacting electron gas; here $T_F \approx 6 \times 10^5$ K $r_s^{-2}$).

Many band structure calculations for hydrogen at various levels of sophistication have been reported [2, 10, 11], but they treat the system as being at $T = 0$ K and numerical values for the electrical conductivity $\sigma$ cannot easily be calculated. Explicit $\sigma$ calculations were only performed in the context of more approximate treatments of electrons and ionic structure and dynamics. All these schemes are inspired by plasma theory and geared towards

the high-temperature, high-density monatomic liquid ($\Gamma \approx 0.1$–10). Stevenson and Ashcroft have applied Ziman's theory to fully ionized dense conducting liquids including hydrogen [12]. Their treatment was later expanded to include temperature and dynamic effects more faithfully [13]. Hansen and McDonald [14] have performed molecular dynamics (MD) simulations of the classical two-component plasma (TCP), where ions and electrons interact with pseudopotentials which differ from the bare Coulomb potential. Perrot and Dharma-wardana derive similar inter-particle pseudopotentials from approximate density functional theories (DFT), but then use hypernetted chain theory to treat the ionic structure [15]. Ichimaru and Tanaka [16] have developed an elaborate scheme for numerical simulations of the electron scattering process in the random fields of the ions, considering also quantum statistical effects on the electron distribution. More recently, a thermodynamic Green function approach has been combined with generalized hydrodynamic theory, to calculate dynamical conductivities under the inclusion of self-consistent localization effects [17].

## 2. Method and computational details

These calculations make various assumptions about the electron–ion, ion–ion and/or electron–electron interaction which make them unsuitable in the density–temperature regime targeted here. Covalent chemical bonds, electron localization and details of the ionic structure play an important role in the vicinity of the molecular–atomic and insulator–metal transition. A method that calculates conductivities quantitatively, treats electron–ion and electron–electron interactions quantum mechanically and that makes no *a priori* assumptions about ion–ion forces and the ionic structure (an *ab initio* method), would be highly desirable. In this contribution we use MD to generate ionic trajectories and compute the forces acting on the classical ions

$$M_I \ddot{\boldsymbol{R}}_I = -\nabla_{R_I} E_{DFT} \tag{1}$$

from first principles using Hohenberg–Kohn–Sham density functional theory (DFT) [18] in the local approximation (LDA). The electronic structure is obtained with little additional effort.

To compute such *ab initio* trajectories we use the Car–Parrinello method [19], for which numerous reviews are available [20]. The fictitious masses $\mu_i$ (for the electronic wave functions $\psi_i$) and the time step sizes $\Delta t$ range from $\mu = 800$ au and $\Delta t = 4$ au at $r_s = 1.5$ to $\mu = 30$ au and $\Delta t = 1$ au at $r_s = 1$. A double Nosé thermostat for the ionic and electronic subsystems was used to avoid the well known non-adiabaticity problems in microcanonical simulations for the larger $\mu$ and $\Delta t$ values [21]. We use cubic or nearly cubic orthorhombic unit cells with periodic boundary conditions containing 96 ($r_s = 1.5$) and 128 ($r_s = 1.3$, 1) hydrogen atoms. Samples of this size can still be thermally equilibrated in a few ps of simulated time, the maximum trajectory length attainable with our computer resources. Larger samples require longer equilibration runs (e.g. 10–15 ps with 250 particles at $r_s = 1$ and 3000 K) and are currently not practical within a full DFT–MD treatment. The plane wave cut-off energy $E_{cut}$ in the expansion of the $\psi_i$ was 50 Ryd. The electron–ion interaction is represented by Martins–Troullier type local pseudopotentials [22] with matching radii of $r_{match} = 0.3$ au and 0.2 au. We found this approach advantageous from a technical point of view over using the bare Coulomb interaction. Optimal $E_{cut}$ and $r_{match}$ combinations were selected from test calculation on the hydrogen molecule and various atomic crystal structures at $r_s = 1$. The Car–Parrinello method has been used very successfully in high-density hydrogen before [23–26].

Several (4–10) statistically independent configurations along carefully thermally equilibrated trajectories were selected, and the frequency dependent conductivity computed with the Kubo–Greenwood formula [27]

$$\sigma(\omega) = \frac{2\pi e^2 \overline{h}^2}{m^2 \Omega} \sum_i \sum_f \left(a_f - a_i\right) \left|\left\langle E_i \left| \partial_x \right| E_f \right\rangle\right|^2 \delta\left(E_f - E_i - \overline{h}\omega\right) \tag{2}$$

representing transitions between occupied initial (here Kohn–Sham LDA) and unoccupied final states $i$ and $f$. The occupation numbers $a$ should be treated as Fermi–Dirac distributions, but we assume the temperature to be low enough compared with the Fermi temperature $T_F$ that we set all $a_i = 2$ and all $a_f = 0$. The $\delta$ function can be resolved by averaging over a finite frequency interval $\Delta\omega$, giving

$$\sigma(\omega) = \frac{2\pi e^2 \overline{h}^2}{m^2 \Omega} \frac{1}{\overline{h}\Delta\omega} \sum_i \sum_f \frac{|\langle E_i | \partial_x | E_f \rangle|^2}{E_f - E_i}. \tag{3}$$

Equation (2) is, in principle, a very general formulation for the conductivity. It contains electron–phonon and electron–electron scattering (the latter inasmuch as it is contained in our model, DFT–LDA). Its implementation in the current study necessitates a number of approximations. (i) Using a $T = 0$ Fermi–Dirac distribution for the electrons amounts to treating electron scattering in the relaxation time approximation and also implies that for any non-zero band gap (always the case in a finite system calculation with discrete energy levels, see (iv)), $\sigma(\omega \to 0)$ will show increasing statistical scatter and eventually quickly and unphysically fall to zero. Therefore the DC conductivity $\sigma(\omega = 0)$ has to be calculated extrapolating from finite $\omega$. We use a Drude formula for this extrapolation; its use will be justified and the error estimated below. (ii) We include a limited number of unoccupied states in our calculation (70–100, covering in excess of $E_{cond} = 3$ Hartree au), and the available range of energy differences between occupied and unoccupied molecular orbitals in our calculations limits $\omega$ from above. $\sigma(\omega)$ will fall off artificially fast for $\omega > E_{cond}$. We have included a sufficiently large number of states for this effect to play no role here. Our principal goal is the static (DC) conductivity. (iii) A potentially problematic approximation is the usage of the electronic density of states (EDOS) obtained from LDA calculations. The underestimation of the band gap is a well-known problem when using DFT–LDA to calculate optical excitations. (iv) Finally, we restrict ourselves to sampling one special $k$-point ($k = 0$ in all MD simulations, and $k = 0$ or $k = [\frac{1}{4}, \frac{1}{4}, \frac{1}{4}]$ (the Baldereschi point [28]) in calculating the EDOS) in the Brillouin zone of the supercell containing typically only some hundred electrons. This has characteristic consequences for the EDOS, as both over- and underestimation of band gaps is possible (see section 3).

Despite these approximations, the current study represents a sophisticated attempt to calculate conductivities in fluid high-density hydrogen. Both thermal (ionic) and electronic structure effects are incorporated at a high level of theory, and no empirical parameters enter our calculations. The procedure outlined above with all its approximations generally yields results that are within 20–30% of available experimental conductivities [29]. Only one other very similar study on hydrogen has come to our attention [30], but covers a different density–temperature regime.

## 3. Results and discussion

In figure 2 we present the frequency-dependent conductivity $\sigma(\omega)$ for $r_s = 1.5$ (a), 1.3 (b), and 1 (c) at $T = 3000$ K in 'raw' data form and fitted to a Drude formula. The errors for

$\omega \to 0$ are too large at the lower temperatures to allow a reliable extrapolation of $\sigma_{DC}$. This is simply a manifestation of the substantial suppression of finite size effects at higher temperature due to Fermi surface smearing. We have fitted both $\sigma_{DC}$ and the relaxation time $\tau$ separately in a simple two-parameter fit to the Drude expression

$$\sigma(\omega) = \frac{\sigma_{DC}}{1 + \tau^2\omega^2} \tag{4}$$

for the data shown. The resulting $\sigma_{DC}$ and $\tau$ values can be found in table 1. The error made in the extrapolation at $T = 3000$ K is not more than about 25% (see figure 2). Fitting a Drude formula, of course, assumes that hydrogen is a free-electron metal to a good approximation at all densities investigated here. Within the statistical errors that they carry, our data do not support a very different conclusion, and the Drude model provides a simple physically motivated extrapolation. At $r_s = 1.5$ one must suspect the opening of an electronic gap as the temperature is lowered towards 0 K, and much better statistics in conjunction with a non-parametric extrapolation of $\sigma(\omega)$ will be necessary to observe the corresponding drop in $\sigma$ as $\omega$ approaches zero. Not surprisingly, the Drude formula provides a better fit to our data with increasing density and, equivalently, metallicity (figure 2). But even at $r_s = 1$, noticeable deviations from ideal free-electron behaviour exist. It is evident from figure 2 and table 1 that there is a clear trend towards higher values of $\sigma$ with increasing density $\sigma \sim \rho^k = (N/V)^k$, $k > 0$. This is what all conductivity models predict, though the individual models differ in $k$ ($k = 1$ in the Drude model, $k = 1/2$ in the Born treatment of fully ionized plasma, $k = 4/3$ in [13]). In reality, of course, one may expect a complex functional behaviour $\sigma(\rho)$ because of ionic structural, chemical and electron localization effects. We observe a more than twelvefold increase in $\sigma$ for a threefold increase in $\rho$.

**Table 1.** DC conductivities $\sigma_{DC}$ (in $10^5\ \Omega^{-1}\ \mathrm{cm}^{-1}$) and relaxation times $\tau$ (in au) from the Drude fit equation (4) for various $r_s$ values at 3000 K.

| $r_s$ | $\sigma_{DC}$ | $\tau$ |
|---|---|---|
| 1.5 | 0.13[a] | 3.0 |
| 1.3 | 0.24 | 4.0 |
| 1 | 1.6 | 6.0 |

[a] Exp.: $0.02 \times 10^5\ \Omega^{-1}\ \mathrm{cm}^{-1}$ [4].

All our samples are in the fluid phase with self-diffusion constants ranging from $D \sim 1.5 \times 10^{-3}$ ($r_s = 1.5$, 3000 K) to $D \sim 1 \times 10^{-4}$ cm$^2$ s$^{-1}$ ($r_s = 1$, 800 K) [23, 24]. While it is easy to define the terms 'conductor' and 'insulator' at zero temperature (the former having a finite value for $\sigma$, the latter having $\sigma = 0$), such definition must be based on the magnitude of $\sigma$ in the fluid phase at finite $T$. For the alkalis, the non-metal–metal borderline can be placed at about $2 \times 10^3\ \Omega^{-1}\ \mathrm{cm}^{-1}$ [31]. Using this criterion, hydrogen is already clearly metallic at $r_s = 1.5$ and 3000 K. Experimentally [4], the conductivity increases sharply with density up to $\rho = 0.31$ mol cm$^{-3}$ and then plateaus at about 2000 $\Omega^{-1}$ cm$^{-1}$ up to 0.36 mol cm$^{-3}$, the end of the measurement range. Our simulations at $r_s = 1.5$ ($\rho = 0.40$ mol cm$^{-3}$) yield a conductivity value (see table 1) of the same order of magnitude but about a factor of six larger. We attribute most of this discrepancy to the pressure–density mismatch between our calculations and the shock experiments (see figure 1), and to the experimental uncertainty in measuring temperature. The error in $\sigma_{DC}$ (table 1) from sampling only $k = 0$ is estimated to be less than 30% everywhere by comparing with selected evaluations of equation (2) at the Baldereschi point

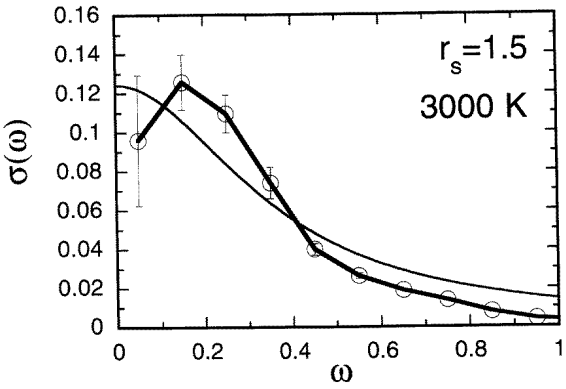


(a)

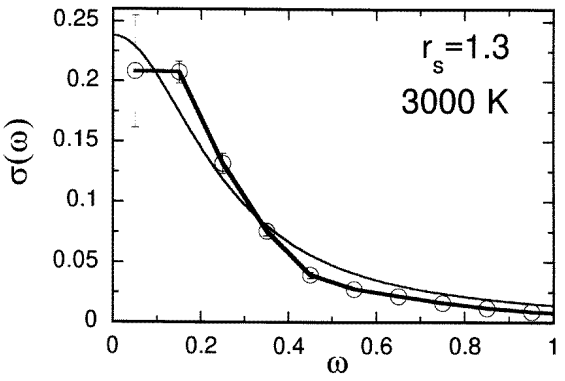


(b)

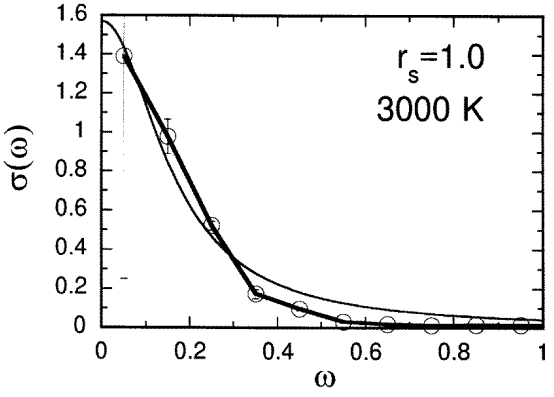


(c)

**Figure 2.** Frequency-dependent electrical conductivity $\sigma(\omega)$ for (a) $r_s = 1.5$, (b) $r_s = 1.3$ and (c) $r_s = 1$ at 3000 K (thick line) and Drude fit (equation (4)) to the data (thin line). $\sigma$ is given in units of $10^5\ \Omega^{-1}\ \mathrm{cm}^{-1}$, $\omega$ in Hartree au. The error bars represent statistical errors only; systematic errors are discussed in the text.

**Table 2.** Average lifetime $\tau_{H_2}$ (in fs) of pairs of atoms, i.e. two atoms within a shell that contains one neighbour in $g(r)$, at various densities and temperatures $T$ (in K).

| $r_s$ | $T$ | $\tau_{H_2}$ |
|---|---|---|
| 1.5 | 800 | 250 |
| | 1400 | 30 |
| | 3000 | 8 |
| 1.3 | 800 | 20 |
| | 3000 | 5 |
| 1 | 800 | 25 |
| | 3000 | 10 |

$k = [\frac{1}{4}, \frac{1}{4}, \frac{1}{4}]$ [28]. As a consistency check, we have also computed $\sigma_{DC}$ with the same procedure in a sample of 216 atoms with $k = 0$ at 3000 K, and again obtain values within 30% of the results with 96 atoms.

We can also compare our numbers with the simulation described in [30], where a very similar theoretical approach is used at higher temperatures. As expected for a metal, $\sigma_{DC}$ falls with increasing temperature (from $1.6 \times 10^5\ \Omega^{-1}\ \mathrm{cm}^{-1}$ at 3000 K (table 1) to $6.65 \times 10^4\ \Omega^{-1}\ \mathrm{cm}^{-1}$ at about 16 000 K [30], at $r_s = 1$). The effect of temperature on $\sigma$ for $T < 3000$ K is too weak to be identifiable within the errors in our own calculations.

It is of great interest to identify the 'mechanism' (i.e. ionic structural changes and/or changes in electronic structure) of the hydrogen metallization (see, e.g. [32]). The central question is whether metallic hydrogen in the vicinity of the transition is still molecular or already dissociated (atomic). Our simulations offer a direct view of the atomic and electronic structure, and we can correlate the increase in conductivity between $r_s = 1.5$ and 1.0 with such changes. The pair correlation function $g(r)$ at $r_s = 1.5$ (see figure 3(a)) shows the progression from a molecular phase consisting of distinguishable $H_2$ molecules at 800 K to a dissociated phase at 3000 K. At 800 K a sharp first peak in $g(r)$ at about $r = 1.5$ au, containing one neighbour represents intramolecular distances; the broad maximum centred around 3.3 au arises from H–H distances between $H_2$ molecules. Already at 1400 K (not shown) the first maximum and minimum in $g(r)$ appear much less pronounced, and at 3000 K, $g(r)$ has the flat featureless form (figure 3(a)) known from simulations of the one-component plasma (OCP) at low values of the Coulomb coupling constant $\Gamma$ [33].

Obviously, intra- and intermolecular distances overlap with one another and with distances between these and other components present in the sample (atoms, filaments [23, 24]). One often sought quantity, the 'dissociation fraction' [4, 5] (implying the proportion of molecules that have dissociated into atoms), is not well defined at these high densities. A simple distance criterion can be applied and is meaningful when a pronounced intramolecular peak is present such as at $r_s = 1.5$ and 800 K. One may still define as 'molecules' all pairs of atoms with distances $d \leqslant r_1$, the value of $r$ up to which $g(r)$ integrates to exactly 1 ($r_1 \approx 1.89$, 1.77 and 1.41 au for $r_s = 1.5$, 1.3 and 1 at 3000 K, respectively). At $r_s = 1.5$, when averaged over the entire trajectory, 96%, 70% and 58% of all atoms in the samples at 800, 1400 and 3000 K, respectively, are 'onefold coordinated' in this way. One may conclude that the dissociation fraction is therefore 4%, 30% and 42%. These numbers are in qualitative agreement with free energy models fitted to available experimental data [5], and the sample appears mainly molecular. This picture is too simplified, and more insight is provided by the average lifetime $\tau_{H_2}$ of a thus defined pair. When these become comparable to, or shorter than, the period of

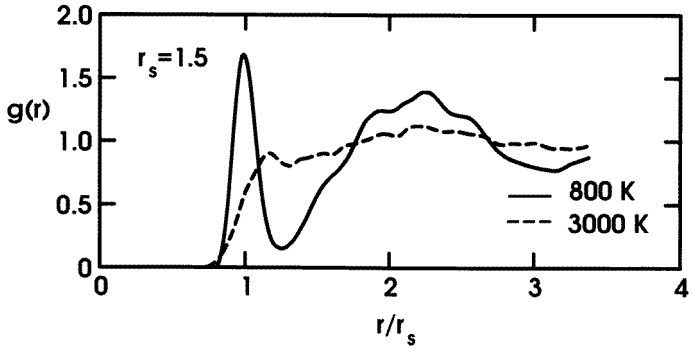


(a)

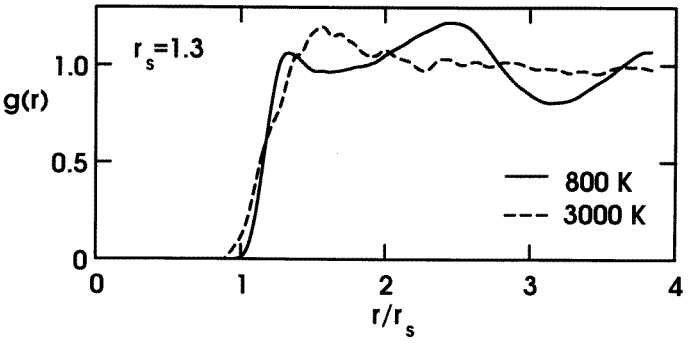


(b)

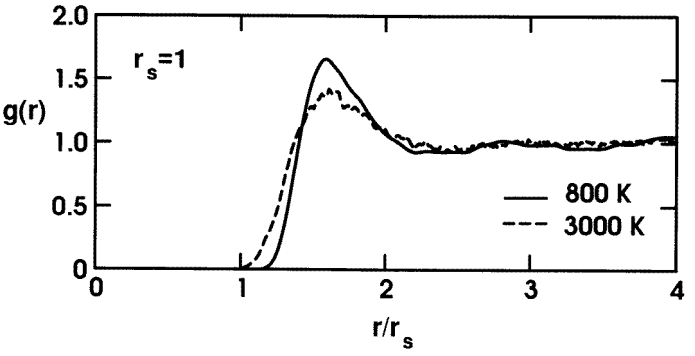


(c)

**Figure 3.** Interproton pair correlation functions $g(r)$ at temperatures of 800 and 3000 K plotted against $r/r_s$ (in au) in hydrogen at (a) $r_s = 1.5$, (b) 1.3 and (c) 1.0.

the fastest phonons ($\approx$4000 cm$^{-1}$ or $8 \times 10^{-15}$ s, the values in the free $H_2$ molecule) it becomes meaningless to speak of 'molecules'. Short-lived close approaches of pairs of atoms are just fluctuations as a result of thermal motion and have nothing to do with the $H_2$ molecule known from chemistry. In table 2 we show the '$H_2$' lifetimes calculated from our simulations (microcanonical and Nosé canonical trajectories lead to virtually identical results). Except at $r_s = 1.5$ and 800 K, pairs of atoms are very short lived, and the samples

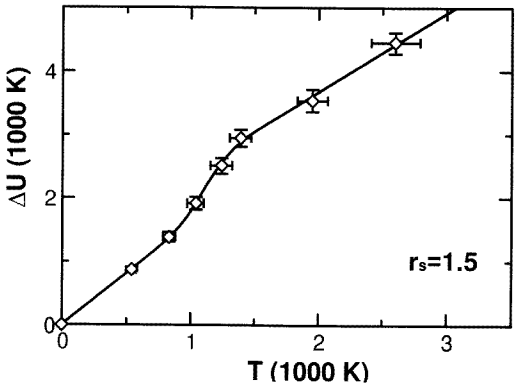


**Figure 4.** Plot of the average potential energy $\Delta U(T)$ (normalized so that $\Delta U(0) = 0$), as a function of temperature (both in units of $10^3$ K) in our MD simulation of $r_s = 1.5$. The measured values (diamonds) are obtained as averages over the trajectories; the error bars represent statistical errors. The solid line is a simple five-parameter fit to the data using a standard form for $U(T)$ near finite-size broadened first-order phase transitions [34]. In the fit, the specific heats $a_1^+$ and $a_1^-$ above and below the transition at $T_c$ were chosen to be different: $c_v(T) = a_1^{\pm} + a_2 \exp[-(T-T_c)^2/a_3^2]$. Our analysis shows that the transition around $T_c = 1100$ K is from a molecular phase of hydrogen to a dissociated phase. Such transition is not observed at $r_s = 1.3$ and 1 (see text).

should not be considered 'molecular' at all. Considerable dissociation of molecules sets in at 1000 K and is complete at 3000 K at $r_s = 1.5$. We can determine the transition temperature $T_c$ by plotting the potential energy $U$ as a function of temperature (see figure 4), and obtain $T_c = 1100$ K for $r_s = 1.5$ ($r_s = 1.3$ and 1 are atomic already at low $T$)†. All our computer samples in the metallic phase at 3000 K are therefore properly described as atomic, contrary to [4, 32]. The models used in [4, 32] are too simple to describe such a complex fluid.

It is also interesting to monitor the changes in electronic structure as the density increases (see figure 5). By doing so, we can also gain insight into the electronic finite size effects. At all $r_s$ values the LDA electronic density of states (EDOS) at 3000 K is more diffuse than at 800 K. The electronic eigenvalues are smeared out by thermal motion, a physical effect. As the density increases the EDOS becomes more and more 'free-electron-like', i.e. resembles a plane wave spectrum in the same MD box (dotted vertical lines in figure 5). This effect is most visible at $r_s = 1$. It becomes immediately clear that finite size effects have substantial influence on the electronic structure. One cannot distinguish 'true' gaps between occupied and unoccupied states from 'artificial' gaps incurred by the finite size of the sample. This also leads to a certain arbitrariness in the occupation numbers for the electronic states. Up to temperatures of about 1000 K, this induces characteristic variations in the geometric structure and $g(r)$ functions (the 'flat' $g(r)$ at $r_s = 1$ and 800 K in figure 3(c) is an example). An interesting discussion of electronic and structural finite size effects deep in the metallic phase of hydrogen can be found in [25]. The smearing of the Fermi surface by thermal motion suppresses these effects sufficiently at 3000 K for equation (2) to become applicable.

† The order of phase transitions is difficult to determine in computer simulations like this one, where a thorough scaling analysis is computationally too expensive. We observe very little hysteresis in figure 4 (not larger than the error bars), which provides some evidence that the transition may be continuous.

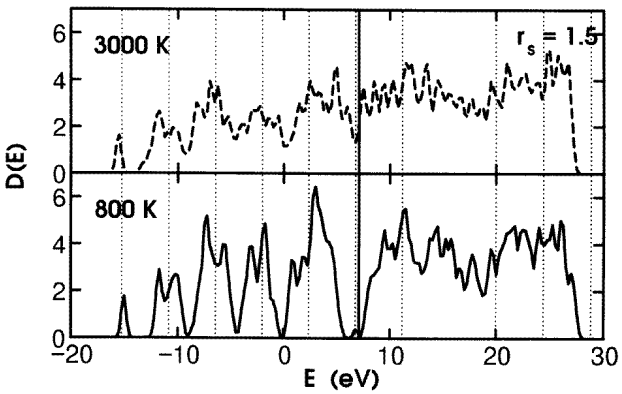


(a)

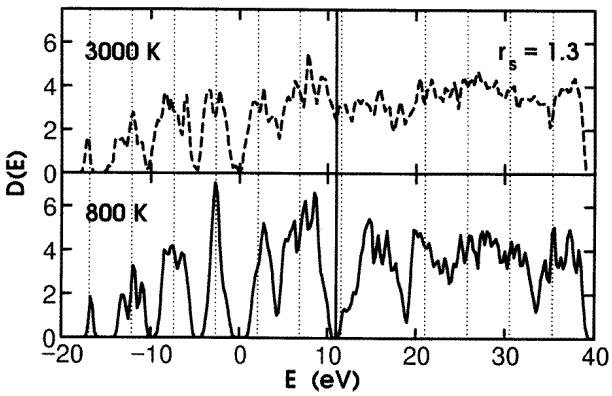


(b)

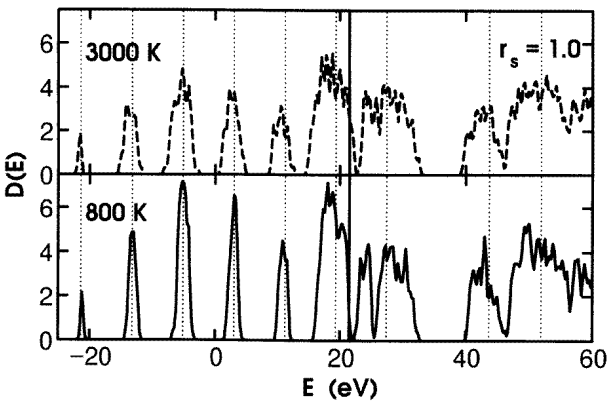


(c)

**Figure 5.** LDA electronic density of states $D(E)$ for (a) $r_s = 1.5$, (b) 1.3, and (c) 1.0 at 800 K (bottom) and 3000 K (top) calculated at $k = \Gamma$. The solid vertical line is the Fermi energy. The dashed vertical lines indicate the position of free-electron bands in an equivalent simple cubic unit cell.

## 4. Conclusions

We have used Car–Parrinello *ab initio* molecular dynamics (AIMD) and a Kubo–Greenwood formulation to analyse structure and conducting behaviour in hot fluid hydrogen for $r_s = 1$–1.5. At 3000 K, where we can calculate conductivities with sufficient accuracy and compare with experimental measurements, hydrogen is clearly metallic at all these densities. Within the inherent statistical errors, the frequency dependency of the conductivity $\sigma(\omega)$ is well described by a simple Drude model. An analysis of the atomic structure and dynamics shows that the metallic samples at 3000 K are all atomic, not molecular. This contradicts prior analyses of experimental data based on empirical free-energy models of hydrogen [4, 32].

We have also gained better insight into applicability of AIMD to electronic properties in metallic systems in general. The most serious source of inaccuracies in the present calculations is the finite size of the electronic systems or, equivalently, the strictly limited $k$-space sampling. Electronic properties such as conductivity are more affected than ionic structure. A substantial improvement over our present one-$k$-point calculations would probably require the inclusion of many hundreds or even thousands of atoms. Such an improved calculation with substantially higher resolution could provide much sought information about the transition from a semiconducting phase at lower densities and temperatures to the metallic phase investigated here.

## Acknowledgments

We thank P Ballone for much active help and many very useful discussions. Our thanks also go to L Collins, J Kress, I Kwon, M Ross and W E Nellis for helpful suggestions and for making data available prior to publication. OP thanks Los Alamos National Laboratories' T-4 Theory Division for their hospitality. DH thanks H C Anderson and his group for their hospitality and useful discussions.

## References

[1] Wigner E and Huntington H B 1935 *J. Chem. Phys.* **3** 764
[2] Mao H K and Hemley R J 1994 *Rev. Mod. Phys.* **66** 671
Silvera I 1992 *Arkhimedes* **44** 108 and references therein
[3] Cui L, Chen N H and Silvera I 1995 *Phys. Rev. Lett.* **74** 4011
[4] Weir S T, Mitchell A C and Nellis W J 1996 *Phys. Rev. Lett.* **76** 1860
[5] Nellis W J, Ross M and Holmes N C 1995 *Science* **269** 1245
[6] Chabrier G, Saumon D, Hubbard W B and Lunine J I 1992 *Astrophys. J.* **391** 817
Saumon D and Chabrier G 1991 *Phys. Rev.* A **44** 5122
Saumon D and Chabrier G 1992 *Phys. Rev.* A **46** 2084 and references therein
[7] Holmes N C, Ross M and Nellis W J 1995 *Phys. Rev.* B **52** 15 835
[8] Hemley R J *et al* 1990 *Phys. Rev.* B **42** 6458
[9] Loubeyre P *et al* 1996 *Nature* **383** 702
[10] Chacham H and Louie S G 1991 *Phys. Rev. Lett.* **66** 64
[11] Kaxiras E, Broughton J and Hemley R J 1991 *Phys. Rev. Lett.* **67** 1138
[12] Stevenson D J and Ashcroft N 1974 *Phys. Rev.* A **9** 782
[13] Stevenson D J and Salpeter E E 1977 *Astrophys. J. Suppl. Ser.* **35** 221
Stevenson D J and Salpeter E E 1977 *Astrophys. J. Suppl. Ser.* **35** 239
[14] Hansen J P and McDonald I R 1981 *Phys. Rev.* A **23** 2041
[15] Perrot F and Dharma-wardana M W C 1987 *Phys. Rev.* A **36** 238
[16] Ichimaru S and Tanaka S 1985 *Phys. Rev.* A **32** 1790
[17] Berkovsky M A 1995 *Physica* A **214** 461

[18] For a review, see Jones R O and Gunnarsson O 1989 *Rev. Mod. Phys.* **61** 689
[19] Car R and Parrinello M 1985 *Phys. Rev. Lett.* **55** 2471
[20] For reviews see: Remler D K and Madden P A 1990 *Mol. Phys.* **70** 921
Pastore G, Smargiassi E and Buda F 1991 *Phys. Rev.* A **44** 6334
Oguchi T and Sasaki T 1991 *Prog. Theor. Phys. Suppl.* **103** 93
Payne M C, Teter M P, Allan D C, Arias T A and Joannopoulos J D 1992 *Rev. Mod. Phys.* **64** 1045
Galli G and Parrinello M 1991 *Computer Simulation in Materials Science* ed M Meyer and V Pontikis (New York: Plenum) p 283
Hohl D 1995 *Theor. Chim. Acta* **91** 237
[21] Blöchl P E and Parrinello M 1992 *Phys. Rev.* B **45** 9413
[22] Troullier N and Martins J L 1991 *Phys. Rev.* B **43** 1993
[23] Pfaffenzeller O 1997 *PhD Thesis* Forschungszentrum Jülich
[24] Hohl D, Natoli V, Ceperley D M and Martin R M 1993 *Phys. Rev. Lett.* **71** 541 and references therein
[25] Kohanoff J and Hansen J P 1995 *Phys. Rev. Lett.* **74** 626
Kohanoff J and Hansen J P 1995 *Phys. Rev.* E **54** 768
[26] Pfaffenzeller O, Hohl D and Ballone P 1995 *Phys. Rev. Lett.* **74** 2599
[27] Kubo R 1957 *J. Phys. Soc. Japan* **12** 570
Greenwood D A 1958 *Proc. Phys. Soc.* A **71** 585
see also Harrison W A 1970 *Solid State Theory* (New York: McGraw-Hill)
[28] Baldereschi A 1973 *Phys. Rev.* B **7** 5212
[29] Kaschner R, Schöne M, Seifert G and Pastore G 1995 *J. Phys.: Condens. Matter* **8** L653
[30] Kwon I, Collins L, Kress J and Troullier N 1996 *Phys. Rev.* E **54** 2844
[31] Mott N F 1990 *Metal–Insulator Transition* (London: Taylor and Francis)
[32] Ross M 1996 *Phys. Rev.* B **54** R9589
[33] see e.g. Hansen J P 1973 *Phys. Rev.* A **8** 3096
[34] Allen M P 1993 *Computer Simulation in Chemical Physics* ed M P Allen and D J Tildesley (Dordrecht: Kluwer) p 49